Simulation of a temperature-compensated palladium-based fiber optic hydrogen sensor and comparison with measurements

Fabian Buchfellner*[a], Qiang Bian[a,b], Alexander Röhrl[a], Fan Zhang[c], Wenbin Hu[c], Minghong Yang[c], Alexander W. Koch[b], Johannes Roths[a]
[a]Photonics Lab, Munich University of Applied Sciences, Munich 80335, Germany;
[b]Institute for Measurement Systems and Sensor Technology, Technical University Munich, Munich 80333, Germany;
[c]National Engineering Research Center for Optical Fiber Sensing Technology, Wuhan University of Technology, Wuhan 430070, China

ABSTRACT

A temperature-compensated sensor architecture for a fiber optic hydrogen sensor consisting of a partly palladium-coated pi-shifted fiber Bragg grating was modeled and compared with measurements. The transfer matrix formalism was used to calculate the spectral line shape of the pi-shifted FBG with a hydrogen-induced, non-homogeneous strain distribution along the grating axis. The temperature response of the grating itself can be compensated by referencing the notch to the flank wavelength. In addition, the hydrogen solubility in Pd shows a non-linear temperature dependence that was also included in the sensor performance calculations. For the investigated H_2 concentration range of 200 ppm to 20000 ppm and between 15 °C and 40 °C, measurement data fit well to the simulation above 3000 ppm but become diffuse below, indicating deviations from the expected dependence according to Sieverts' square root law.

Keywords: Hydrogen sensing, Pi-shifted fiber Bragg grating, temperature-compensation, coupled mode theory

1. INTRODUCTION

Palladium (Pd) and its alloys have convinced as an extremely suitable material for hydrogen (H_2) gas sensing due to its exceptional H_2 sorption characteristics at room temperature[1]. For fiber optic H_2 sensing, Pd-coated fiber Bragg gratings (FBGs) were reported with two fundamentally different sensing mechanisms: refractive index sensing by surface plasmons with Pd-coated tilted FBGs[2] and FBG strain sensing due to volumetric expansion of Pd films during H_2 absorption[3, 4]. Both techniques have the potential for precise sub-% H_2 gas sensing with fast sorption times and good selectivity, especially towards CH_4[1].

Nonetheless, the particular limiting factor for measurement accuracy is temperature, where two temperature effects manifest the bottleneck of both sensing mechanisms. These effects include i) the intrinsic temperature coefficient of the FBG itself due to thermal expansion and thermo-optic refractive index changes[5] and ii) the temperature-dependent solubility of the Pd thin film that results in declining H_2 sensitivities with increasing temperature[6].

Mitigation of those temperature-enabled, non-discernible wavelength shifts of the FBGs is of paramount importance for real-field applications. Cai et al.[2] have referenced their H_2- and temperature-dependent optical cladding mode to the temperature-dependent core mode to overcome the temperature response of a tilted FBG. Our research group[7, 8] has recently reported on experimental studies with a PSFBG, where only a small section – that included the pi shift of the grating – was covered with a Pd alloy thin film. This allowed referencing the notch wavelength of the narrow transmission window to the flank wavelength of the broader reflection band in the PSFBG spectrum, where temperature-induced wavelength shifts ideally appear equally at both notch and flank, but H_2-induced wavelength shifts particularly occur at the notch as only this grating section is covered with Pd.

With this work, we report on a simulation based on the coupled mode theory and the transfer matrix algorithm[9] to model the recently proposed partly Pd-coated temperature-compensated sensor architecture. Input parameters for H_2-induced strains that are coupled from the volumetric expansion of the Pd thin film onto the fiber were computed with Sieverts' law[10]. A comparison of measurement data and simulated curves revealed good agreement. This model offers a helpful toolset to optimize Pd-based FBG sensors in general and particularly our temperature-decoupled PSFBG H_2 sensor.

*fabian.buchfellner0@hm.edu; phone +49 1265 3654; http://fk06.hm.edu/pol/en/index.html

2. SENSOR ARCHITECTURE AND MODEL

The investigated sensor configuration consisted of a 10-mm-long PSFBG and a centered 4-mm-long coating, as shown in Fig. 1a. The coating consisted of four layers, a 10 nm Ni adhesion layer, a 200 nm Pd_{91}:Ni_9 sensitive layer, a 40 nm Pd_{50}:Pt_{50} catalytic layer, and a 40 nm PTFE protection layer. Alloying Pd with Ni prevents the measurement at low concentrations (<2 vol.%) from undesired hysteresis[6].

Modeling the spectrum of a PSFBG can be achieved with the coupled mode theory and transfer matrices (TMs)[9] by stringing two uniform FBGs together with a propagation distance of $\pi = m\lambda/2$ in between. For the spectrum of a partly Pd-coated PSFBG, where only a fraction of the full grating is subject to H_2-induced strains, but all sections are subject to temperature, the model consists of two more uniform sections, as shown in the schematic in Fig. 1a. Here, the outer two uniform TMs do not experience strain ($\varepsilon = 0$) but temperature (ϑ). The inner two uniform TMs and the propagation distance TM experience both temperature and H_2-induced strain. The TM for a uniform FBG can be found from Erdogan[9], where the complete PSFBG-TM is given by the multiplication of each section $T_{PSFBG} = \prod_i T_i$. The spectra can then be derived by the ratio $R(\lambda, \varepsilon, \vartheta) = \left|T_{PSFBG,12}/T_{PSFBG,22}\right|^2$. TMs of each section require the input parameters[11]

$$\Delta n_{AC,i}(\vartheta, \varepsilon_i) = [1 - p_e\varepsilon_i(c_i) + \alpha_n\vartheta]\Delta n_{AC,0}, \tag{1}$$

$$n_{eff,i}(\vartheta, \varepsilon_i) = [1 - p_e\varepsilon_i(c_i) + \alpha_n\vartheta]n_{eff,0}, \tag{2}$$

$$L_i(\vartheta, \varepsilon_i) = [1 - \varepsilon_i(c_i) + \alpha_{CTE}\vartheta]L_{i,0}, \tag{3}$$

$$\Lambda_i(\vartheta, \varepsilon_i) = [1 - \varepsilon_i(c_i) + \alpha_{CTE}\vartheta]\Lambda_0, \tag{4}$$

where $\Delta n_{AC,i}$ is the refractive index modulation amplitude, $n_{eff,i}$ is the effective refractive index, L_i is the length, Λ_i is the grating pitch of each i-th section, p_e is the elasto-optic coefficient, α_n the thermo-optic coefficient, and α_{CTE} is the thermal expansion coefficient. H_2-induced strains $\varepsilon_i(c_i)$ are computed under the plane-strain assumption, i.e., only strains along the fiber axis occur. The strain coupling factor $k_{f\leftrightarrow Pd}$ between fiber and Pd thin film is given by[3]

$$k_{f\leftrightarrow Pd} = \frac{A_{Pd}Y_{Pd}}{A_fY_f + A_{Pd}Y_{Pd}}, \tag{5}$$

where Y_{Pd}, Y_f are Young's moduli of Pd and fiber, r_f is the fiber radius, and d_{Pd} the thickness of the coating. Sieverts' law[10] describes the solution of gases in metals as

$$n_H = \sqrt{c}/K(\vartheta), \tag{6}$$

where n_H denotes the atomic ratio of H to Pd atoms within the thin film, c is the H_2 concentration in the gas phase, and $K(\vartheta)$ is the temperature-dependent Sieverts' constant, given by[12]

$$K(\vartheta) = \exp\left[-\frac{\Delta H^0}{2R(273 + \vartheta)} + \frac{\Delta S^0}{2R}\right], \tag{7}$$

with ΔH^0 being the molar enthalpy, ΔS^0 the molar entropy and R the gas constant.

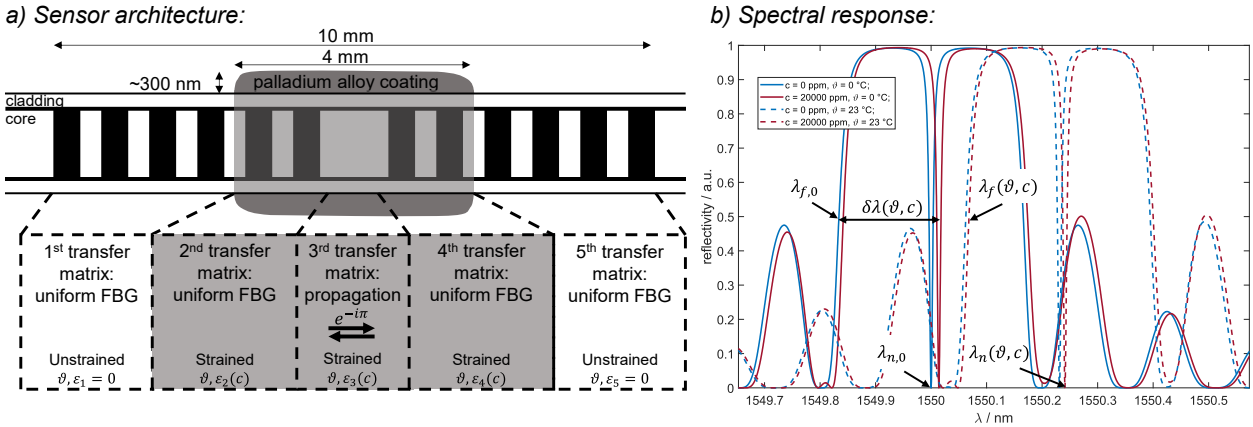

Figure 1: Sensor architecture and spectral response of a partly Pd-coated pi-shifted FBG and a visualization of the model approach with the pi-shifted FBG consisting of five sections (two strained uniform sections and a strained propagation section due to H_2 sorption and two unstrained uniform sections).

The H_2-induced strain is then[3]

$$\varepsilon(c) = \Delta L/L = C \cdot k_{f\leftrightarrow Pd} \cdot n_H, \tag{8}$$

with a scaling factor C that is derived from the characteristic volume change per H-atom[12]. After calculation of the TMs for all sections and of the complete PSFBG spectra at different concentrations and temperatures, the notch and flank wavelengths, $\lambda_n(\vartheta, c)$ and $\lambda_f(\vartheta, c)$, are extracted, and the spectral distance $\delta\lambda(\vartheta, c)$ between notch and flank can be calculated according to

$$\delta\lambda(\vartheta, c) = \Delta\lambda_n(\vartheta, c) - \Delta\lambda_f(\vartheta, c), \tag{9}$$

where $\Delta\lambda$ denotes the wavelength shift $\lambda(\vartheta, c) - \lambda_0(0,0)$ with respect to the wavelength λ_0 at 0 °C and no strain. Corresponding simulated spectra are shown in Fig. 1b at 0 °C/0 ppm (blue, solid), 0 °C/20000 ppm (red, solid), 23 °C/0 ppm (blue, dashed), and 23 °C/20000 ppm (red, dashed). Comparing the solid lines, i.e., spectra at equal temperature but different H_2 concentration, the notch wavelength $\lambda_n(\vartheta, c)$ undergoes a slightly larger shift than the flank wavelength $\lambda_f(\vartheta, c)$. Comparing the blue solid to the blue dashed line, i.e., spectra at different temperatures but without H_2 exposure, the spectrum has ideally shifted as a whole. Therefore, referencing the notch to the flank wavelength, i.e., building the spectral distance $\delta\lambda(\vartheta, c)$, allows to compensate the temperature response of the PSFBG itself. Contrarily, comparing the notch wavelength shifts between H_2 absence and exposure at each temperature, i.e., blue solid with red solid and blue dashed with red dashed, the notch wavelength shift due to H_2 at 23 °C is less than at 0 °C. This indicates the temperature-dependent H_2 solubility, where with increasing temperature, less H_2 can be dissolved in the Pd, leading to less volumetric expansion and to reduced strain coupled onto the PSFBG.

3. RESULTS AND CONCLUSIONS

Parameters to compute Eqs. (1)-(9) are summarized in Table 1, and the simulation results for the wavelength shifts as functions of H_2 concentrations are plotted in Figs. 2a for $\Delta\lambda_n(\vartheta, c)$, in 2b for $\Delta\lambda_f(\vartheta, c)$, and in 2c for $\delta\lambda(\vartheta, c)$ as solid lines. Colors indicate different temperatures that were chosen according to the measurement data shown in Fig. 2c (dashed). Measurements were conducted with the procedure described in our previous work[7] for concentrations between 200 ppm and 20000 ppm. By comparison of Figs. 2a and 2b, it is evident that both the notch and the flank of the PSFBG sensor are subject to H_2-induced wavelength shifts, although the flank is less sensitive. The sensitivity of the spectral distance $\delta\lambda(\vartheta, c)$ shown in Fig. 2c is approx. 1/2 of the notch sensitivity. To achieve the largest sensitivity difference between notch and flank to optimize the sensitivity of $\delta\lambda(\vartheta, c)$, the coating-to-grating length ratio should be further reduced, as reported by Hu et al.[8]. Comparison of simulated (solid) and measured (dashed) data in Fig. 2c reveals a clear discrepancy at low concentrations, where the measurement becomes diffuse and apparently not follows Sieverts' square root law in Eq. (6). We assume that this is due to the insufficient temperature stability of the experimental setup, where pure N_2 and pre-mixed 2 vol.% H_2/N_2 are dynamically mixed, and temperature drifted slightly between hydrogen exposure and absence (i.e., the solubility of the Pd film changed slightly during mixing). Hence, improvements in temperature stabilization during measurements are required. Apparently, found from both the model and measurements is the declining wavelength response to H_2 when temperatures increase. Although the notch wavelength is referenced to the flank wavelength in $\delta\lambda(\vartheta, c)$, which efficiently compensates for the temperature response of the PSFBG itself, the temperature coefficient in the H_2 solubility remains and hence limits the sensor performance if not considered during data procession, for instance by means of an iterative matrix algorithm[7].

Table 1. Parameters used for the transfer matrix model to compute a PSFBG with strained and unstrained grating sections.

Parameter		**Value**	**Ref.**	**Parameter**		**Value**	**Ref.**
Index modulation	$\Delta n_{AC,0}$	$2\text{x}10^{-4}$		Fiber radius	r_f	62.5 µm	
Eff. refractive index	$n_{eff,0}$	1.4479	[11]	Young's mod. of fiber	Y_f	73.1 GPa	[11]
Grating length	$L_{PSFBG,0}$	10 mm		Coating thickness	d_{Pd}	240 nm	
Grating pitch	Λ_0	535 µm		Coating length	$L_{Pd,0}$	4 mm	
Elasto-optic coeff.	p_e	0.211	[11]	Young's mod. of Pd	Y_{Pd}	128 GPa	[13]
Thermo-optic coeff.	α_n	$5.66\text{x}10^{-6}$ K^{-1}	[11]	Molar enthalpy	ΔH^0	4620 cal mol^{-1}	[12]
Th. expansion coeff.	α_{CTE}	$0.55\text{x}10^{-6}$ K^{-1}	[11]	Molar entropy	ΔS^0	25.5 cal mol^{-1} K^{-1}	[12]
Gas constant	R	1.987 cal mol^{-1} K^{-1}	[12]	Scaling factor	C	0.063	[12]

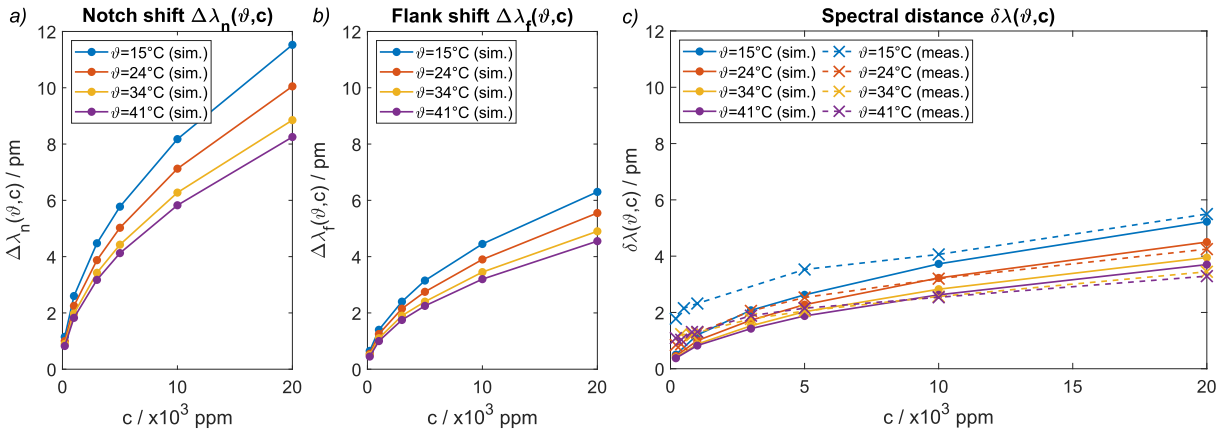

Figure 2: Wavelength responses vs. H_2 concentration for a) the notch wavelength shift $\Delta\lambda_n(\vartheta, c)$, b) the flank wavelength shift $\Delta\lambda_f(\vartheta, c)$, and c) the spectral distance between notch and flank $\delta\lambda(\vartheta, c)$. Colors indicate different temperatures, solid lines are simulation results, and dashed lines represent measured curves.

In conclusion, this work represents a method to model the wavelength response of a Pd-coated PSFBG hydrogen sensor by linking the coupled mode theory and the transfer matrix formalism with Sieverts' law and a plane-strain approach. This configuration is capable of compensating for the intrinsic temperature response of the grating by referencing the notch wavelength to the flank wavelength of the PSFBG. Nonetheless, simulation and measurement have indicated that the temperature dependence of the Pd solubility has a high misreading potential if not considered during data evaluation. Simulation results and measurement curves deviate at H_2 concentrations below 3000 ppm, which is assumed to rather be an experimental issue. The proposed model can help to design robust Pd-based FBG sensors and to optimize the sensor performance over a broad H_2 concentration and temperature range.

Funding: Deutsche Forschungsgemeinschaft (448330062); Nat. Natural Science Foundation of China (62061136002)

REFERENCES

[1] Wienecke, M., Lengert, M., Weidner, M., Ciudin, R., Heeg, J., Frank, T. and Kienke, P. (eds.), [Pd based MEMS Hydrogen Sensors], VDE (2022).

[2] Cai, S., Liu, F., Wang, R., Xiao, Y., Li, K., Caucheteur, C. and Guo, T., "Narrow bandwidth fiber-optic spectral combs for renewable hydrogen detection," Sci. China Inf. Sci. 63(12) (2020).

[3] Sutapun, B., "Pd-coated elastooptic fiber optic Bragg grating sensors for multiplexed hydrogen sensing," Sensors and Actuators B: Chemical 60(1), 27–34 (1999).

[4] Dai, J., Yang, M., Yu, X., Cao, K. and Liao, J., "Greatly etched fiber Bragg grating hydrogen sensor with Pd/Ni composite film as sensing material," Sensors and Actuators B: Chemical 174, 253–257 (2012).

[5] Kersey, A. D., Davis, M. A., Patrick, H. J., LeBlanc, M., Koo, K. P., Askins, C. G., Putnam, M. A. and Friebele, E. J., "Fiber grating sensors," J. Lightwave Technol. 15(8), 1442–1463 (1997).

[6] Sakamoto, Y., Matsuo, T., Sakai, H. and Flanagan, T. B., "Absorption of Hydrogen by Palladium — Nickel Alloys," Zeitschrift für Physikalische Chemie 162(1), 83–96 (1989).

[7] Buchfellner, F., Bian, Q., Hu, W., Hu, X., Yang, M., Koch, A. W. and Roths, J., "Temperature-decoupled hydrogen sensing with Pi-shifted fiber Bragg gratings and a partial palladium coating," Opt. Lett., OL 48(1), 73 (2023).

[8] Hu, X., Hu, W., Dai, J., Ye, H., Zhang, F., Yang, M., Buchfellner, F., Bian, Q., Hopf, B. and Roths, J., "Performance of Fiber-Optic Hydrogen Sensor Based on Locally Coated π -Shifted FBG," IEEE Sensors J. 22(24), 23982–23989 (2022).

[9] Erdogan, T., "Fiber grating spectra," J. Lightwave Technol. 15(8), 1277–1294 (1997).

[10] Sieverts, A., "Absorption of gases by metals," Zeitschrift für Metallkunde 21, 37–46 (1929).

[11] Marchi, G., Stephan, V., Dutz, F. J., Hopf, B., Polz, L., Huber, H. P. and Roths, J., "Femtosecond Laser Machined Micro-Structured Fiber Bragg Grating for Simultaneous Temperature and Force Measurements," J. Lightwave Technol. 34(19), 4557–4563 (2016).

[12] Alefeld, G. and Vökl, J. (eds.), [Hydrogen in metals], Springer, Berlin (1978).

[13] Masumoto, H., Sawaya, S. and hachi, "The Thermal Expansion Coefficient and the Temperature Coefficient of Young's Modulus of Nickel-Palladium and Nickel-Platinum Alloys," Trans. JIM 11(6), 391–394 (1970).